ISSN: 0256-307X

中国物理快报
Chinese Physics Letters

Volume 28 Number 12 December 2011

A Series Journal of the Chinese Physical Society
Distributed by IOP Publishing

Online: http://iopscience.iop.org/cpl
http://cpl.iphy.ac.cn

CHINESE PHYSICAL SOCIETY
Institute of Physics PUBLISHING

Tunable Single-Frequency Intracavity Frequency-Doubled Ti:Sapphire Laser around 461 nm *

LI Feng-Qin(李凤琴)**, SHI Zhu(石柱), LI Yong-Min(李永民), PENG Kun-Chi(彭堃墀)

State Key Laboratory of Quantum Optics and Quantum Optics Devices, Institute of Opto-Electronics Shanxi University, Taiyuan 030006

(Received 24 August 2011)

We demonstrate a tunable continuous-wave single frequency intracavity frequency-doubled Ti:sapphire laser. The highest output power of 280 mW at 461.62 nm is obtained by employing a type-I phase-matched BIBO crystal and the peak-to-peak fluctuation of the power is less than ±1% within three hours. The frequency stability is better than ±2.22 MHz over 10 min when the laser is locked to a confocal Fabry–Perot cavity. A three-plate birefringent filter allows for the tunable range from 457 nm to 467 nm, which covers the absorption line of the strontium atoms (460.86 nm).

PACS: 42.60.By, 42.60.Lh, 42.65.Ky DOI:10.1088/0256-307X/28/12/124205

All-solid-state continuous-wave blue lasers have wide applications in biomedicine, high-density optical data storage, high-resolution spectroscopy, laser cooling, etc. It is known that atomic clocks operating at optical rather than microwave frequencies have higher accuracy and stability.[1] Because of the narrow transition width of the strontium atom, the accuracy of the time can be highly enhanced[2] and the strontium atoms have been widely used in optical clock systems. For laser cooling and trapping, the dipole transition between the $^1S_0$ and $^1P_1$ states of the strontium atoms at 461 nm is usually adopted. Thus a single frequency and tunable high power light at 461 nm is desired in a strontium optical clock. Blue light at 461 nm has been generated by external cavity frequency doubling of a tapered amplified 922 nm diode laser.[3,4] Adopting the similar scheme, a commercial product which can deliver 220 mW blue light at 461 nm has been developed by the TOPTICA Co. However, owing to the poor beam quality of the diode laser, generated blue lasers show poor spatial profiles. Compared with diode lasers, Ti:sapphire lasers have some merits such as wide tunable range, superior beam quality, low noise and long coherent length. Recently, about 200 mW blue light at 461 nm has been achieved by external cavity frequency doubling of Ti:sapphire lasers.[5,7] It is known that intracavity frequency doubling can take advantage of the high intracavity circulating laser power without the need of active electronic stabilization of the laser cavity. At the same time, the size of the laser source can be reduced greatly. In this Letter, we present a blue light source at 461 nm by intracavity frequency doubling of a Ti:sapphire laser. Output power of 280 mW at 461.62 nm is achieved at the incident pump power of 8 W at 532 nm. The frequency fluctuation is less than ±2.22 MHz in 10 min when the laser is actively locked to a confocal Fabry–Perot (F-P) cavity.[8–10] The blue laser can be tuned from 457 to 467 nm with birefringent filters and the tuning range is wide enough to cover the absorption line of the strontium atoms.

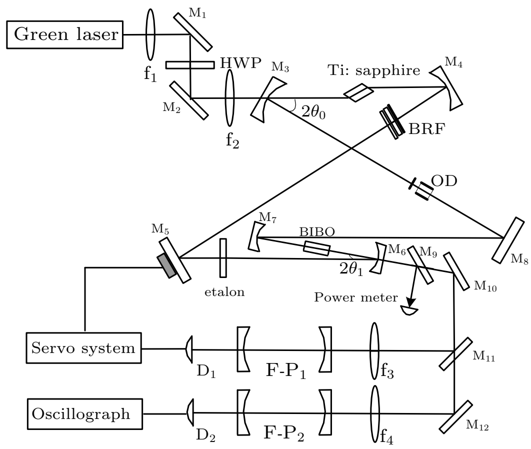

Fig. 1. Schematic diagram of the experimental setup.

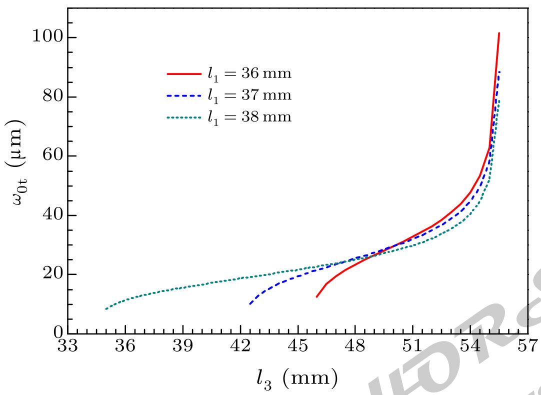

Fig. 2. The waist size at the center of the Ti:sapphire crystal as a function of the distance between M_6 and $M_7(l_3)$ with different l_1.

Figure 1 shows the schematic diagram of the experimental setup. The pump source is a high power all-solid-state single frequency green laser (YUGUANG

*Supported by the National Natural Science Foundation of China under Grant No 60821004, and the National High-tech R&D Program of China (2011AA030203).
**Correspondence author. Email: lfq@sxu.edu.cn

Co. Ltd.), whose output power is more than 8 W and the central wavelength is 532 nm. The green laser is focused on the Ti:sapphire crystal by two plano-convex lenses. The cylindrical Ti:sapphire crystal with a diameter of 5 mm and a length of 10 mm is 0.05 wt% doped. It has an absorption coefficient of 1.05 cm^{-1} at 532 nm, whose figure of merit (FOM) is more than 275. The Brewster-angle-cut Ti:sapphire is wrapped with indium foil and mounted on a water-cooled copper holder, the temperature of the water is stabilized at 14.5℃. The c-axis of the Ti:sapphire is set to be vertical to the optical path. By adjusting the half wavelength plate in front of the cavity, the π-polarized 532 nm green laser is well absorbed by the Ti:sapphire crystal. An astigmatically compensated double-folded resonator is employed to give two tight-focus regions, where the Ti:sapphire and BIBO crystals are located. The spacing between M3 and Ti:sapphire crystal is l_1. Mirrors M_3 and M_4 have radii of curvature of 75 mm. M_6 and M_7 have radii of curvature of 50 mm and spacing of l_3. M_3 is high-reflection at 922 nm ($R > 99.9\%$) and high-transmission at 532 nm ($T > 90\%$).M_4, M_5 and M_8 are high-reflection at 922 nm ($R > 99.9\%$). M_7 is high-reflection at 922 nm and 461 nm ($R > 99.9\%$). M_6 is high-reflection at 922 nm ($R > 99.9\%$) and high-transmission at 461 nm ($T > 90\%$). The Ti:sapphire crystal is placed in the middle of M_3 and M_4, where a small astigmatism-compensated beam waist is located. To compensate for the astigmatism of the cavity, the fold angle θ_0 of 17.5° is used. The second fold angle θ_1 is made as small as possible to be about 3.5° without the beam blocking. In order to avoid spatial hole-burning, the unidirectional operation is maintained with an optical diode consisting of an 8-mm-long terbium gallium garnet (TGG) rod followed by an AR-coated zeroth-order half-wave plate (HWP) at 922 nm. A three-plate birefringent filter (BRF), with length of 1 mm, 2 mm and 4 mm, is inserted for frequency tuning. When tuning the laser, rotation of the HWP is found to be crucial to maximize the output and maintain a stable unidirectional operation. An uncoated thin etalon with thickness of 0.5 mm is used to ensure a single longitudinal mode operation of the laser.

We employ a type-I phase-matched BIBO crystal as the nonlinear crystal to reduce the waveplate behavior. The BIBO crystal is a relatively new nonlinear crystal which belongs to the monoclinic borate family.[11] It has a much higher nonlinear coefficient than that of LBO, and can be type-I phase-matched at room temperature at 922 nm. Considering the walk-off effect, a relatively shorter BIBO crystal with dimensions of 3 mm × 3 mm × 6 mm is used in our experiment. It is dual band AR-coated at 922/461 nm. The crystal is also wrapped with an indium foil and mounted in a temperature-controlled copper oven. Using a thermoeletrical temperature controller with accuracy of 0.01℃, the temperature of the BIBO crystal is stabilized to the optimal value of 42.7℃. Due to the large difference of the birefringence ratio, the phase matching of the BIBO crystal is sensitive to the change of the fundamental wavelength. Thus we fix the copper oven on a θ–Φ–xyz translation stage positioned at the center between M_6 and M_7. The total round-trip distance of the resonator is about 703 mm. To achieve a high optical to optical conversion efficiency, the pumping-to-oscillating mode matching and the doubling efficiency are very important.[12] The calculated waist sizes of the oscillating mode in the Ti:sapphire (ω_0) and the BIBO (ω_1) crystals as functions of l_1 and l_3 are shown in Figs. 2 and 3, respectively. From the theoretical results, M_3 and the Ti:sapphire crystal are separated by 37 mm (l_1) in the experiment, where the waist size (ω_1) in the BIBO crystal is relatively small to ensure a high doubling efficiency. The spacing of M_6 and $M_7(l_3)$ is set to the center of the resonator stability region, where the waist size (ω_0) in the Ti:sapphire crystal is insensitive to the change of cavity length. When the astigmatism is compensated for, ω_0 is formed to be about 38 µm(sagittal plane)×37 µm(tangential plane) and ω_1 is formed to be about 30.2 µm(sagittal plane)×29.5 µm(tangential plane). According to the requirement of the optimal pumping to oscillating mode matching in the cw Ti:sapphire laser,[13] the spot size of the pump laser(ω_p) is adjusted to be about 22 µm by means of two lenses with focal length of 200 and 100 mm.

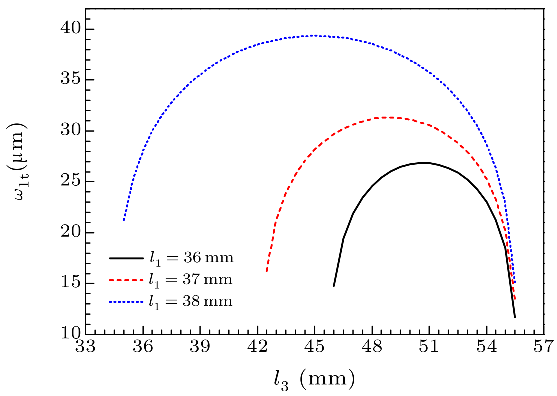

Fig. 3. The waist size at the center of the BIBO crystal as a function of the distance between M_6 and $M_7(l_3)$ with different l_1.

The maximum output power of the single frequency blue laser at 461.62 nm is measured to be 280 mW, corresponding to an optical to optical conversion efficiency of 3.5%. The output power of the blue laser at 461.62 nm as a function of the incident pump power is shown in Fig. 4. The peak-to-peak fluctuation of the maximum power in three hours is about ±1%, as shown in Fig. 5. Because the coatings of all the cavity mirrors are specially coated for high reflectivity at 922 nm to enhance the doubling efficiency, the tuning of the blue laser is limited to the range from 457 nm to 467 nm, as shown in Fig. 6. When the wavelength is tuned close to the absorption line of the strontium (460.86 nm), the measured output power is about 202 mW. Due to the walk-off effect of the BIBO crystal, the emitted blue beam is elliptical in shape.

The frequency drift of the freely running blue laser in 10 s is about ±3.55 MHz. After the laser is locked on a confocal F-P cavity with an electronic servo-system, the frequency stability of the blue laser is better than ±556 kHz in 10 s and ±2.22 MHz in 10 min in the total tuning range, as shown in Figs. 7(a) and 7(b).

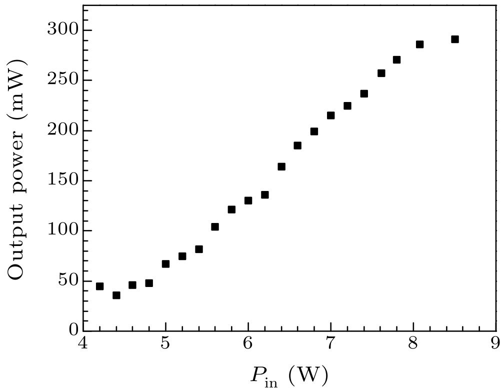

Fig. 4. The output power of the blue laser at 461.62 nm as a function of pump power.

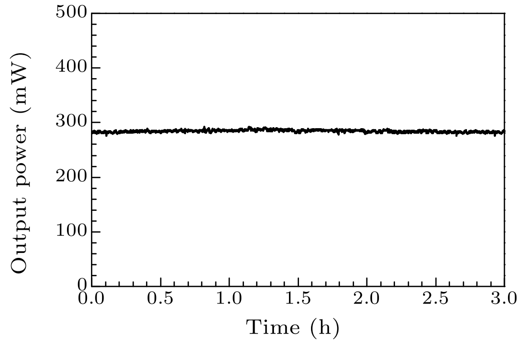

Fig. 5. Power fluctuation of the blue laser in three hours.

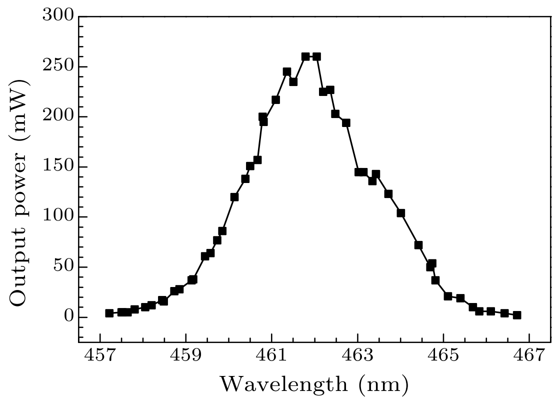

Fig. 6. Tuning curve of the single frequency Ti:sapphire blue laser.

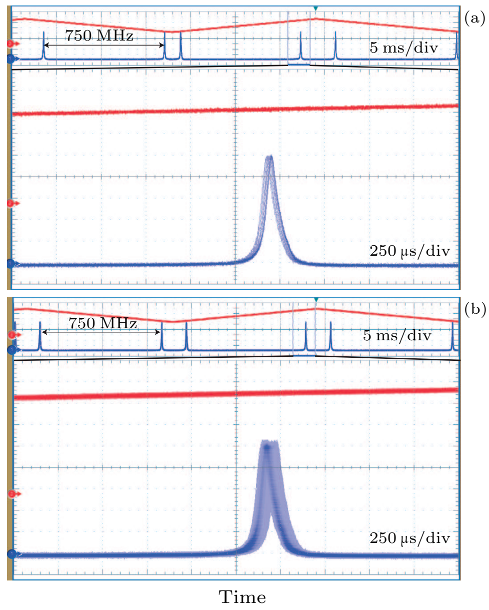

Fig. 7. The frequency drift when the laser is locked to the reference cavity. (a) Observation time of 10 s, (b) observation time of 10 min.

In summary, we have demonstrated a stable cw tunable single-frequency intracavity frequency-doubled Ti:sapphire laser around 461 nm. Using a type-I phase-matched BIBO as the nonlinear crystal, the maximum output of 280 mW at 461.62 nm is obtained, corresponding to an optical-to-optical conversion efficiency (532–461 nm) of 3.5%. The blue laser can be tuned from 457 nm to 467 nm. By locking the laser to a confocal F-P cavity, the frequency fluctuation decreases to ±2.22 MHz in 10 min. The blue laser presented here can be applied to laser cooling and trapping in the strontium optical clock system.

References

[1] Huang B Y 2006 *New Generation Atomic Clocks* (Wuhan: Wuhan University Press) p 1 (in Chinese)
[2] Takamoto M et al 2003 *Phys. Rev. Lett.* **91** 223001
[3] Schwedes C et al 2003 *Appl. Phys.* B **76** 143
[4] Targat R L et al 2005 *Opt. Commun.* **247** 471
[5] Aaron D S 2005 PhD Dissertation (Houston: Rice University) (in American)
[6] Ye L et al 2008 *Conference on Precision Electromagnetic Measurements Digest* (Broomfield, CO 8–13 June 2008) 190
[7] Vainio M et al 2011 *Appl. Phys.* B **104** 897
[8] Zhao F G et al 2004 *Chin. Opt. Lett.* **2** 334
[9] Peng K C et al 1985 *Appl. Opt.* **24** 938
[10] Chang D X et al 2008 *Chin. J. Lasers* **35** 323
[11] Wang Z P et al 2003 *Acta Phys. Sin.* **52** 2176 (in Chinese)
[12] Lv B D *Laser Optics* (Beijing: Higher Education Press) p 386 (in Chinese)
[13] Anthony J A 1989 *IEEE J. Quantum Electron.* **25** 760

Chinese Physics Letters

Volume 28 Number 12 December 2011

GENERAL

120201 **Conservation Laws and Self-Consistent Sources for a Super-Classical-Boussinesq Hierarchy**
YU Fa-Jun

120202 **Poisson Theory and Inverse Problem in a Controllable Mechanical System**
XIA Li-Li

120301 **Quantum Entanglement Channel based on Excited States in a Spin Chain**
ZHANG Shao-Liang, DU Liang-Hui, GUO Guang-Can, ZHOU Xing-Xiang, ZHOU Zheng-Wei

120302 **Non-Markovian Dynamics of Quantum and Classical Correlations in the Presence of System-Bath Coherence**
LI Chuan-Feng, WANG Hao-Tian, YUAN Hong-Yuan, GE Rong-Chun, GUO Guang-Can

120303 **An Effective Heisenberg Spin Chain in a Fiber-Cavity System**
ZHONG Zhi-Rong, ZHANG Bin, LIN Xiu, SU Wan-Jun

120304 **Manipulating Quantum State in Superconducting Dressed-State Systems**
ZHANG Feng-Yang, PEI Pei, LI Chong, SONG He-Shan

120305 **New Aspects of Field Entropy Squeezing as an Indicator for Mixed State Entanglement in an Effective Two-Level System with Stark Shift**
S. Abdel-Khalek, M. M. A. Ahmed, A-S F. Obada

120306 **Quantum Key Distribution Based on a Weak-Coupling Cavity QED Regime**
LI Chun-Yan, LI Yan-Song

120307 **Quantum Memory via Wigner Crystals of Polar Molecules**
XUE Peng

120308 **Arbitrary and Fast Quantum Gate with Semiconductor Double-Dot Molecules on a Chip**
ZOU Wei-Ping, ZHANG Gang, XUE Zheng-Yuan

120401 **Gödel-Type Universes in $f(R)$ Gravity with an Arbitrary Coupling between Matter and Geometry**
ZHANG Tao, WU Pu-Xun, YU Hong-Wei

120501 **Scattering Behavior of Waveguide Channels of a New Coupled Integrable Dispersionless System**
Abbagari Souleymanou, Victor K. Kuetche, Thomas B. Bouetou, Timoleon C. Kofane

120502 **Frequency Effect of Harmonic Noise on the FitzHugh–Nagumo Neuron Model**
SONG Yan-Li

120503 **Projective Synchronization of Complex Dynamical Networks with Time-Varying Coupling Strength via Hybrid Feedback Control**
GUO Xiao-Yong, LI Jun-Min

120504 **Projective Synchronization in Modulated Time-Delayed Chaotic Systems Using an Active Control Approach**
FENG Cun-Fang, WANG Ying-Hai

120505 **Hurst's Exponent Determination for Radial Distribution Functions of In, Sn and In-40 wt%Sn Melt**
ZHOU Yong-Zhi, LI Mei, GENG Hao-Ran, YANG Zhong-Xi, SUN Chun-Jing

120506 **Exact Solution of the Gyration Radius of an Individual's Trajectory for a Simplified Human Regular Mobility Model**
YAN Xiao-Yong, HAN Xiao-Pu, ZHOU Tao, WANG Bing-Hong

120507 **Fractal Analysis of Transport Properties in a Sinai Billiard**
JIANG Guo-Hui, ZHANG Yan-Hui, BIAN Hong-Tao, XU Xue-You

120508 **Backstepping-Based Synchronization Control of Cross-Strict Feedback Hyper-Chaotic Systems**
LI Hai-Yan, HU Yun-An

120701 **Fast Nondestructive Identification of Endothelium Corneum Gigeriae Galli Using Visible/Near-Infrared Spectroscopy**
ZHANG Xiao-Yan, MENG Yao-Yong, ZHANG Hao, OU Wen-Juan, LIU Song-Hao

THE PHYSICS OF ELEMENTARY PARTICLES AND FIELDS

121101 **Virial Relation for Compact Q-Balls in the Complex Signum-Gordon Model**
WANG Hua-Wen, CHENG Hong-Bo

121301 **Semi-Leptonic and Non-Leptonic B Meson Decays to Charmed Mesons**
FU Hui-Feng, WANG Guo-Li, WANG Zhi-Hui, CHEN Xiang-Jun

121401 **Flavor State of the Neutrino: Conditions for a Consistent Definition**
RONG Shu-Jun, LIU Qiu-Yu

NUCLEAR PHYSICS

122101 **Chiral Doublet Bands with $\nu h_{11/2} \otimes \nu d_{5/2}^{-1}$ Configuration in the Particle Rotor Model**
QI Bin, WANG Shou-Yu, ZHANG Shuang-Quan

122401 **Nuclear Dynamical Quadrupole Deformations in Heavy-Ion Reactions**
DOU Liang, WANG Nan, ZHAO En-Guang

122501 **Two-Pion Interferometry for the Granular Sources in Ultrarelativistic Heavy Ion Collisions at the RHIC and the LHC**
ZHANG Wei-Ning, YIN Hong-Jie, REN Yan-Yu

122502 **Hadronic Transport Effects on Elliptic Flow**
LI Na, SHI Shu-Su

122503 **Fragmentation Functions for Heavy Baryons in the Recombination Model**
PENG Ru

ATOMIC AND MOLECULAR PHYSICS

123201 **Calculation of Ion Equilibrium Temperature in Ultracold Neutral Plasmas**
LI Jin-Xing, CAO Ming-Tao, HAN Liang, QI Yue-Rong, ZHANG Shou-Gang, GAO Hong, LI Fu-Li, T. C. Killian

123401 **Elastic Scattering Properties of Ultracold Strontium Atoms**
ZHANG Ji-Cai, ZHU Zun-Lue, LIU Yu-Fang, SUN Jin-Feng

123402 **Lattice-Inversion Embedded-Atom-Method Interatomic Potentials for Group-VA Transition Metals**
YUAN Xiao-Jian, CHEN Nan-Xian, SHEN Jiang

123403 **Positronium Formation in Positron-Lithium Scattering**
CHENG Yong-Jun, ZHOU Ya-Jun, LIU Fang

123601 **Reverse Polarization of a High-Energy Exciton in Conjugated Polymers**
LI Xiao-Xue, DONG Xian-Feng, GAO Kun, XIE Shi-Jie

FUNDAMENTAL AREAS OF PHENOMENOLOGY(INCLUDING APPLICATIONS)

124101 **Characterizing the Temporal Structure of a Relativistic Electron Bunch**
DENG Hai-Xiao, FENG Chao, LIU Bo, WANG Dong, WANG Xing-Tao, ZHANG Meng

124102 **Transmission Characteristics of a Generalized Parallel Plate Dielectric Waveguide at THz Frequencies**
YE Long-Fang, XU Rui-Min, ZHANG Yong, LIN Wei-Gan

124201 **Peculiar Transmission Characteristics of the Large Gap Semi-Insulating GaAs Photoconductive Switch**
SHI Wei, MA Xiang-Rong

124202 **Nonparaxial Propagation of a Radially Polarized Beam Diffracted by an Annular Aperture**
CHEN Jian-Nong

124203 **Spontaneous Emission Spectrum of a Λ-Typed Atom in a Coherent Photonic Reservoir**
HUANG Xian-Shan, LIU Hai-Lian

124204 **Nanosecond Square Pulse Fiber Laser based on the Nonlinear Amplifying Loop Mirror**
CHEN Guo-Liang, GU Chun, XU Li-Xin, WANG An-Ting, MING Hai

124205 **Tunable Single-Frequency Intracavity Frequency-Doubled Ti:Sapphire Laser around 461 nm**
LI Feng-Qin, SHI Zhu, LI Yong-Min, PENG Kun-Chi

124206 **Compact and Highly Efficient Passively Q-Switched Intracavity KTA-OPO at 1.53 and 3.47 μm**
MIAO Jie-Guang, PAN Yu-Zhai, QU Shi-Liang

124207 **Ghost Imaging Using Orbital Angular Momentum**
ZHAO Sheng-Mei, DING Jian, DONG Xiao-Liang, ZHENG Bao-Yu

124301 **Influence of Ultrasonic Vibrations on the Static Friction Characteristics of a Rubber/Aluminum Couple**
CHENG Ting-Hai, GAO Han, BAO Gang

124401 **Thermal Rectification in Graded Nonlinear Transmission Lines**
XU Wen, CHEN Wei-Zhong, TAO Feng

124701 **In-depth Study on Cylinder Wake Controlled by Lorentz Force**
ZHANG Hui, FAN Bao-Chun, CHEN Zhi-Hua

124702 **Renormalization Group Analysis of Weakly Rotating Turbulent Flows**
WANG Xiao-Hong, ZHOU Quan

124703 **Mini-Jet Controlled Turbulent Round Air Jet**
DU Cheng, MI Jian-Chun, ZHOU Yu, ZHAN Jie

124704 **Wake Oscillator Model Proposed for the Stream-Wise Vortex-Induced Vibration of a Circular Cylinder in the Second Excitation Region**
XU Wan-Hai, DU Jie, YU Jian-Xing, LI Jing-Cheng

124705 **Three-Dimensional Simulation of Detonation Propagation in a Rectangular Duct by an Improved CE/SE Scheme**
SHEN Hua, LIU Kai-Xin, ZHANG De-Liang

124706 **Heat Transfer in a Moving Fluid over a Moving Non-Isothermal Flat Surface**
Swati Mukhopadhyay

124707 **Unsteady Viscous Flow over an Expanding Stretching Cylinder**
FANG Tie-Gang, ZHANG Ji, ZHONG Yong-Fang, TAO Hua

PHYSICS OF GASES, PLASMAS, AND ELECTRIC DISCHARGES

125201 **Sheath Criterion for a Collisional Electronegative Plasma Sheath in an Applied Magnetic Field**
ZOU Xiu, LIU Hui-Ping, QIU Ming-Hui, SUN Xiao-Hang

125202 **Methods of Generation and Detailed Characterization of Millimeter-Scale Plasmas Using a Gasbag Target**
LI Zhi-Chao, ZHENG Jian, JIANG Xiao-Hua, WANG Zhe-Bin, YANG Dong, ZHANG Huan, LI San-Wei, WANG Feng, PENG Xiao-Shi, YIN Qiang, ZHU Fang-Hua, GUO Liang, YUAN Peng, LIU Shen-Ye, DING Yong-Kun

125203 **Korteweg de Vries Description of One-Dimensional Superfluid Fermi Gases**
XU Yan-Xia, DUAN Wen-Shan

CONDENSED MATTER: STRUCTURE, MECHANICAL AND THERMAL PROPERTIES

126101 **Structural and Electronic Properties, and Pressure-Induced Phase Transition of Layered C_5N: a First-Principles Investigation**
HU Qian-Ku, WANG Hai-Yan, WU Qing-Hua, HE Ju-Long, ZHANG Guang-Lei

126102 **First-Principles Study of Fe-Doped ZnO Nanowires**
ZHANG Fu-Chun, ZHANG Wei-Hu, DONG Jun-Tang, ZHANG Zhi-Yong

126103 ***In Situ* High-Pressure Synchrotron X-Ray Diffraction Study of Clinozoisite**
FAN Da-Wei, MA Mai-Ning, YANG Jun-Jie, WEI Shu-Yi, CHEN Zhi-Qiang, XIE Hong-Sen

126201 **Production and Mechanical Behaviour of Biomedical CoCrMo Alloy**
O. Sahin, A. Rıza Tuncdemir, H. Ali Cetinkara, H. Salih Guder, E. Sahin

CONDENSED MATTER: ELECTRONIC STRUCTURE, ELECTRICAL, MAGNETIC, AND OPTICAL PROPERTIES

127101 **Vacancy and H Interactions in Nb**
RAO Jian-Ping, OUYANG Chu-Ying, LEI Min-Sheng, JIANG Feng-Yi

127102 **First-Principles Study of the Local Magnetic Moment on a N-Doped Cu_2O (111) Surface**
WANG Zhi

127201 **Magnetism of a Nitrogen-Implanted TiO_2 Single Crystal**
LIU Chun-Ming, XIANG Xia, ZHANG Yan, JIANG Yong, ZU Xiao-Tao

127202 **Wafer-Scale Gigahertz Graphene Field Effect Transistors on SiC Substrates**
PAN Hong-Liang, JIN Zhi, MA Peng, GUO Jian-Nan, LIU Xin-Yu, YE Tian-Chun, LI Jia, DUN Shao-Bo, FENG Zhi-Hong

127203 **Improved Performance of Pentacene Organic Field-Effect Transistors by Inserting a V_2O_5 Metal Oxide Layer**
ZHAO Geng, CHENG Xiao-Man, TIAN Hai-Jun, DU Bo-Qun, LIANG Xiao-Yu

127301 **Photoresponse Properties of an n-ZnS/p-Si Heterojunction**
HUANG Jian, WANG Lin-Jun, TANG Ke, XU Run, ZHANG Ji-Jun, LU Xiong-Gang, XIA Yi-Ben

127302 **Negative Photoconductivity Induced by Surface Plasmon Polaritons in the Kretschmann Configuration**
ZHENG Jing-Gao, SUN Jia-Lin, XUE Ping

127303 **Surface Potential Equation for Metal-Oxide-Semiconductor Capacitors Considering the Degenerate Effect**
ZHANG Da, SUN Jiu-Xun, PU Jin-Rong

127304 **Single-Walled Carbon Nanotube Networked Field-Effect Transistors Functionalized with Thiolated Heme for NO_2 Sensing**
WEI Ang, LI Wei-Wei, WANG Jing-Xia , LONG Qing, WANG Zhao, XIONG Li, DONG Xiao-Chen, HUANG Wei

127305 **Photovoltaic Behaviors in an Isotype n-TiO_2/n-Si Heterojunction**
FAN Hui-Jie, ZHANG Hui-Qiang, WU Jing-Jing, WEN Zheng-Fang, MA Feng-Ying

127306 **Transparent Conductive Al-Doped ZnO/Cu Bilayer Films Grown on Polymer Substrates at Room Temperature**
HUANG Ji-Jie, WANG Yu-Ping, LU Jian-Guo, GONG Li, YE Zhi-Zhen

127701 **The Evidence for Ferroelectricity on Magnetite Ceramics below the Verwey Transition**
WU Yu-Qiang, WU Hong-Ying, ZHAO Jie, LU Cui-Min, ZHANG Bao-Long, LIU Qing-Suo, MA Yong-Chang

127801 **Temperature and Composition Dependence of $GaN_xAs_{1-x}(0 < x \leq 0.05)$ before and after Annealing**
ZHAO Chuan-Zhen, LI Na-Na, WEI Tong, TANG Chun-Xiao

127802 **Enhancement of Er^{3+} Emission from an Er-Si Codoped Al_2O_3 Film by Stacking Si-Doped Al_2O_3 Sublayers**
WANG Xiao, JIANG Zui-Min, XU Fei, MA Zhong-Quan, XU Run, YU Bin, LI Ming-Zhu, ZHENG Ling-Ling, FAN Yong-Liang, HUANG Jian, LU Fang

CROSS-DISCIPLINARY PHYSICS AND RELATED AREAS OF SCIENCE AND TECHNOLOGY

128101 **Density Increase of Upper Quantum Dots in Dual InGaN Quantum-Dot Layers**
LV Wen-Bin, WANG Lai, WANG Jia-Xing, HAO Zhi-Biao, LUO Yi

128201 **Spectroscopy of a Gamma Irradiated Poly(Acrylic Acid)-Clotrimazole System**
M. Todica, C. V. Pop, Luciana Udrescu, Traian Stefan

128202 **An X-Ray Diffraction and Thermogravimetric Study of Layered Perovskite $Y_{1-x}Bi_xBaCo_4O_7$**
ZHANG Ya-Mei, HAN Ru-Qu, WU Xiao-Shan, WANG Zhi-He

128301 **Herding Effect in Coupled Pedestrian-Pedestrian Interacting Dynamics**
DING Jian-Xun, LING Xiang, HUANG Hai-Jun, TAKASHI Imamura

128401 **Highly Efficient PCDTBT:PC_{71} BM Based Photovoltaic Devices without Thermal Annealing Treatment**
YANG Shao-Peng, KONG Wei-Guang, LIU Bo-Ya, ZHENG Wen-Yao, LI Bao-Min, LIU Xian-Hao, FU Guang-Sheng

128402 **A Dielectric Multilayer Filter for Combining Photovoltaics with a Stirling Engine for Improvement of the Efficiency of Solar Electricity Generation**
SHOU Chun-Hui, LUO Zhong-Yang, WANG Tao, SHEN Wei-Dong, ROSENGARTEN Gary, WANG Cheng, NI Ming-Jiang, CEN Ke-Fa

128501 **Comparison of GaN-Based Light-Emitting Diodes by Using the AlGaN Electron-Blocking Layer and InAlN Electron-Blocking Layer**
CHEN Jun, FAN Guang-Han, PANG-Wei, ZHENG Shu-Wen

128502 **Characteristics and Time-Dependent Instability of Ga-Doped ZnO Thin Film Transistor Fabricated by Radio Frequency Magnetron Sputtering**
HUANG Hai-Qin, SUN Jian, LIU Feng-Juan, ZHAO Jian-Wei, HU Zuo-Fu, LI Zhen-Jun, ZHANG Xi-Qing, WANG Yong-Sheng

128503 **Design of a 1200-V Thin-Silicon-Layer p-Channel SOI LDMOS Device**
HU Sheng-Dong, ZHANG Ling, LUO Xiao-Rong, ZHANG Bo, LI Zhao-Ji, WU Li-Juan

128504 **Unique Properties of Heat Generation in Nanoscale Systems**
ZHOU Li-Ling

GEOPHYSICS, ASTRONOMY, AND ASTROPHYSICS

129801 **Shallow Decay Phase of the Early X-Ray Afterglow from External Shock in a Wind Environment**
LEI Hai-Dong, WANG Jiu-Zhou, LÜ Jing, ZOU Yuan-Chuan

129802 **Gravitational Instability in Neutrino Dominated Accretion Disks**
LIU Tong, XUE Li

ERRATA AND OTHER CORRECTIONS

129901 **Withdrawal of Chinese Physics Letters 28 (2011) 107301 "High-Efficiency Graphene Photo Sensor Using a Transparent Electrode" by LIU Tao and HUANG Zheng**
LIU Tao, HUANG Zheng

129902 **Erratum: Numerical Simulation of Coupled Nonlinear Schrödinger Equations Using the Generalized Differential Quadrature Method**
R. Mokhtari, A. Samadi Toodar, N. G. Chegini

129903 **Author Index to Vol. 28**